PAPER

Structural modal parameter identification using local mean decomposition

IOP Publishing Measurement Science and Technology
Meas. Sci. Technol. **29** (2018) 025003 (12pp) https://doi.org/10.1088/1361-6501/aa97f4

Structural modal parameter identification using local mean decomposition

Ali Keyhani and Saeed Mohammadi

Department of Civil Engineering, Shahrood University of Technology, No. 316, Daneshgah Ave., Shahrood, Iran

E-mail: s.mohammadi@alumni.ut.ac.ir

Received 24 May 2017, revised 19 October 2017
Accepted for publication 3 November 2017
Published 17 January 2018

Abstract

Modal parameter identification is the first step in structural health monitoring of existing structures. Already, many powerful methods have been proposed for this concept and each method has some benefits and shortcomings. In this study, a new method based on local mean decomposition is proposed for modal identification of civil structures from free or ambient vibration measurements. The ability of the proposed method was investigated using some numerical studies and the results compared with those obtained from the Hilbert–Huang transform (HHT). As a major advantage, the proposed method can extract natural frequencies and damping ratios of all active modes from only one measurement. The accuracy of the identified modes depends on their participation in the measured responses. Nevertheless, the identified natural frequencies have reasonable accuracy in both cases of free and ambient vibration measurements, even in the presence of noise. The instantaneous phase angle and the natural logarithm of instantaneous amplitude curves obtained from the proposed method have more linearity rather than those from the HHT algorithm. Also, the end effect is more restricted for the proposed method.

Keywords: local mean decomposition, structural health monitoring, modal parameters identification, time-frequency analysis

(Some figures may appear in colour only in the online journal)

Introduction

Nowadays, there are many important existing structures, such as bridges, towers, and historical buildings, for which comprehensive knowledge about their dynamical properties is necessary for any structural evaluation, control or rehabilitation purposes. Structural system identification is the first step in the structural health monitoring of existing structures during which the dynamical characteristics of the structure, i.e. mass, stiffness, and damping matrices, are obtained. Alternatively, system identification is done through finding natural frequencies, damping ratios, and mode shapes in the modal space through the process named modal parameter identification.

In the traditional system identification methods, i.e. input–output (IO) methods, external excitations and structural responses should both be known. The external excitations that the structure is subjected to in its lifetime are not always measurable, and, on the other hand, applying a synthetic controllable force to the structure is not economical and also compromises the safety of the structure. Therefore, IO methods are applicable in very limited number of cases. In recent years, the output only methods, that is only structural responses are needed for system identification, were taken into consideration as a result of significant developments in signal processing techniques. A brief history of the conventional system identification methods in the time domain is presented in the following.

The Ibrahim time domain (ITD) method (Ibrahim and Mikulcik 1973) is known as the first formulated method for identifying single input–single output systems. The ITD is required to free vibration responses of the structure in all degrees of freedoms. An eigen-system realization algorithm (ERA) (Juang and Pappa 1985) has been used for modal identification and model reduction of a dynamic system from its mathematical model in discrete state space form. A major restriction of classical identification methods such as ITD

and ERA is their requirement of the impact or free vibration response of the structure. To overcome this problem, the natural excitation technique was proposed (James *et al* 1995). Stochastic subspace identification can be used when the structural response is provided from stochastically forced vibration (Abdelghani *et al* 1998). In this method, unknown external forces are assumed to be an uncorrelated stochastic time series.

Kerschen *et al* (2007) developed a set of signal processing techniques, named blind source separation (BSS), to structural system identification. There were two major restrictions for this method: (1) the responses in all DOFs have to be recorded; (2) the structure needs to be un-damped or have very slight damping. These restrictions have been alleviated by different researchers in recent years. A comprehensive review of all BSS-based identification methods with recent developments can be found in Sadhu *et al* (2017).

One of the common assumptions in the above-mentioned identification methods is that the measured outputs are a stationary process, while this is not realistic in some practical cases such as responses recorded during severe earthquakes. Not making this assumption, Huang *et al* (1998) proposed a novel algorithm, named empirical mode decomposition (EMD), that can be used for non-stationary, non-linear time series analysis. Using the EMD method, a signal can be decomposed into a set of intrinsic mode functions (IMFs) where each of them has only one frequency component. This process is followed by a Hilbert transform for each IMF to obtain the corresponding instantaneous phase angle (IP) and instantaneous amplitude (IA). Although Yang *et al* (2003) used the EMD algorithm for system identification, EMD suffers from some problems such as mode mixing and end effects. The mode mixing phenomena can be reduced by band-pass filtering of the original signal in the desired frequency band (Yang *et al* 2003). Moreover, adding several white noises to the original signal before the decomposition process and subtracting them from the IMFs at the end can reduce mode mixing to some extent (Wu and Huang 2009). For the end effect problem, some approaches, such as a mirror extension at the both ends and adding characteristic waves, have been proposed (Huang *et al* 1998, Quek *et al* 2003). Given that the IMFs, by definition, are mono-component signals, the well-behaved Hilbert transform can be applied to them to extract IPs and IAs. Consequently, the natural frequency and the damping ratio of each mode can be calculated with respect to the slope of corresponding IP and IA curves against time. Hazra *et al* (2012) employed the EMD technique successfully for underdetermined blind identification of structures, where the responses in all DOFs were not available. Sadhu (2017) combined multivariate EMD and ensemble EMD to enhance the traditional EMD algorithm with multichannel vibration measurements and to overcome the mode mixing problem. More detail about the traditional EMD algorithm followed by the Hilbert transform, named the Hilbert–Huang transform (HHT), can be seen in Huang *et al* (1998) and Yang *et al* (2003). Recently, a synchrosqueezed wavelet transform (SWT) was employed for modal parameter identification of structures (Perez-Ramirez *et al* 2016, Li *et al* 2017). The studies showed that the SWT can be considered as a serious challenger to the EMD algorithm, especially in the case of noisy and low amplitude measurements.

In the current study, a new method based on a novel signal processing technique, named local mean decomposition (LMD), is proposed for structural system identification. LMD is a self-adaptive time-frequency analysis method, which was first introduced by Smith (2005) for the analysis of electroencephalograms. Similar to EMD, the LMD algorithm decomposes a given signal to a set of mono-component AM–FM signals, named product functions (PFs). Recently, LMD has been successfully used for damage diagnosis of rotating machinery by several researchers (Cheng *et al* 2012, Liu and Han 2014, Xiang and Yan 2014). However, its ability to extract modal parameters of civil structures has not been investigated distinctly. In this study, a new method is proposed in which the LMD algorithm is utilized for modal identification of structures from free or ambient vibrations.

The LMD algorithm

LMD is a self-adaptive time-frequency analysis method whose original purpose was to decompose a multi-component signal to a set of frequency modulated (FM) signals and envelope signals. The product of each FM signal and the corresponding envelope signal is named a PF, which has physical meaning (Liu and Han 2014). The decomposition process based on a standard LMD algorithm for a given signal, say $X(t)$, is described as follows (Liu and Han 2014):

i. Find all the local extrema, n_i, of the signal.
ii. Calculate the local means, m_i, and local amplitudes, a_i, according to equations (1) and (2), respectively:

$$m_i = \frac{n_i + n_{i+1}}{2} \tag{1}$$

$$a_i = \frac{|n_i - n_{i+1}|}{2} \tag{2}$$

then the continuous local mean, $\tilde{m}_{11}(t)$, and local amplitude, $\tilde{a}_{11}(t)$, functions are obtained using moving average tools (Liu and Han 2014).
iii. The local mean function is subtracted from the original signal, and then the residual signal $h_{11}(t)$ can be expressed as equation (3):

$$h_{11}(t) = X(t) - \tilde{m}_{11}(t). \tag{3}$$

$h_{11}(t)$ is divided by the local amplitude function $\tilde{a}_{11}(t)$ to obtain $s_{11}(t) = h_{11}(t)/\tilde{a}_{11}(t)$. If $s_{11}(t)$ is a purely FM signal, then go to the next step. Otherwise, $s_{11}(t)$ is regarded as the original dataset and the two initial steps are repeated until $s_{1q_1}(t) = h_{1q_1}(t)/\tilde{a}_{1q_1}(t)$ is a purely FM signal t oscillates between -1 and 1, where q_1 denotes the number of iterations required to obtain the first PF. This step is the so-called 'sifting process' of the LMD algorithm.

iv. The first PF can be constructed by equation (4):

$$\mathrm{PF}_1(t) = \mathrm{IA}_1(t)s_{1q_1}(t) \tag{4}$$

where $\mathrm{IA}_1(t)$ is the corresponding IA, which is calculated by equation (5):

$$\mathrm{IA}_1(t) = \tilde{a}_{11}(t)\tilde{a}_{12}(t)...\tilde{a}_{1q_1}(t) = \prod_{j=1}^{q_1}\tilde{a}_{1j}(t). \tag{5}$$

Also, the corresponding instantaneous phase (IP), $\mathrm{IP}_1(t)$, and instantaneous frequency (IF), $\mathrm{IF}_1(t)$, can be written as equations (6) and (7), respectively:

$$\mathrm{IP}_1(t) = \arccos\left(s_{1q_1}(t)\right) \tag{6}$$

$$\mathrm{IF}_1(t) = \frac{f_s}{2\pi}\frac{\mathrm{d}(\mathrm{IP}_1(t))}{\mathrm{d}t} \tag{7}$$

where f_s is the sampling frequency.

v. The derived PF from the previous step is subtracted from the original signal, $u_1(t) = X(t) - \mathrm{PF}_1(t)$. Then the residual signal $u_1(t)$ is regarded as the original signal and the above procedure is repeated to extract the next PF until $u_p(t)$ is a monotonic function with no oscillations. Finally, one can obtain

$$X(t) = \sum_{i=1}^{p}\mathrm{PF}_i(t) + u_p(t). \tag{8}$$

Three issues in using the LMD algorithm

The issue of step size selection for the moving average (MA) tool. It should be mentioned that the decomposition results of the LMD method are affected by the step size of the MA for estimating local mean and local amplitude functions. In this study, the following criterion is considered to determine the step size of the MA (Wang *et al* 2009):

$$\Delta = [\max(k_l - k_{l-1})]/\rho \quad l = 2, 3, ..., n_M \tag{9}$$

where Δ is the step size of MA; k_l, n_M are the index of extrema and the number of extrema, respectively; and ρ is a constant that is chosen according to the signal type. For signals with transient components, as in this study, it has been considered as $\rho = 5$ (Wang *et al* 2009).

The end effect issue. The LMD algorithm, similar to EMD, suffers from boundary effects. To improve the performance of the EMD algorithm at the signal ends, some approaches such as mirror extension at both ends and adding characteristic waves have already been proposed (Huang *et al* 1998, Quek *et al* 2003). In this study, an improved mirror extension technique has been used to reduce the end effect issue (Liu *et al* 2017). According to this technique, the mirror point is determined based on the following four rules:

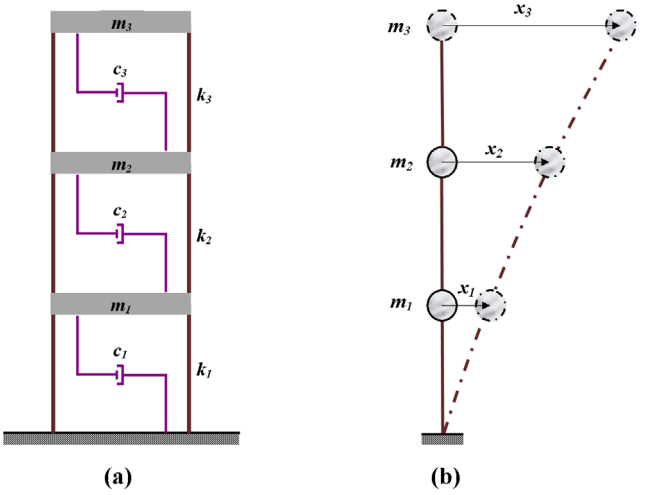

Figure 1. (a) The 3-DOF shear building for the case study (I); (b) its simplified model.

(1) If the first local extrema is a maxima and the signal value at the end point is smaller than the first local minimum, then the mirror point is set to the end point.
(2) If the first local extrema is a maxima and the signal value at the end point is not smaller than the first local minimum, then the mirror point is set to the first local maxima.
(3) If the first local extrema is a minima and the signal value at the end point is greater than the first local maximum, then the mirror point is set to the end point.
(4) If the first local extrema is a minima and the signal value at the end point is not greater than the first local maximum, then the mirror point is set to the first local minima.

The above rules demonstrate how to select the mirror point in the left end of the signal. Similar rules can be used for selecting the mirror point in the right end of the signal. More detail about this technique can be found in Liu *et al* (2017).

The stoppage criterion. According to step (iii) of the LMD algorithm described above, the sifting process is continued until $s_{1q}(t)$ is a purely FM signal that oscillates between -1 and 1. In this study, the following criterion has been used as the stoppage criterion of the sifting process (Liu *et al* 2017):

$$\mathrm{SD} = \mathrm{RMS}(z(n)) + \mathrm{EK}(z(n)) \tag{10}$$

where $z(n) = a(n) - 1$, i.e. the zero base-line envelope signal; $\mathrm{RMS}(z(n))$ and $\mathrm{EK}(z(n))$ are, correspondingly, the root mean square and excess kurtosis of $z(n)$ and defined as equations (11) and (12), respectively:

$$\mathrm{RMS}(z(n)) = \sqrt{\frac{1}{N_s}\sum_{n=1}^{N_s}(z(n))^2} \tag{11}$$

$$\mathrm{EK}(z) = \frac{\frac{1}{N_s}\sum_{n=1}^{N_s}(z(n)-\bar{z})^4}{\left[\frac{1}{N_s}\sum_{n=1}^{N_s}(z(n)-\bar{z})^2\right]^2} - 3 \tag{12}$$

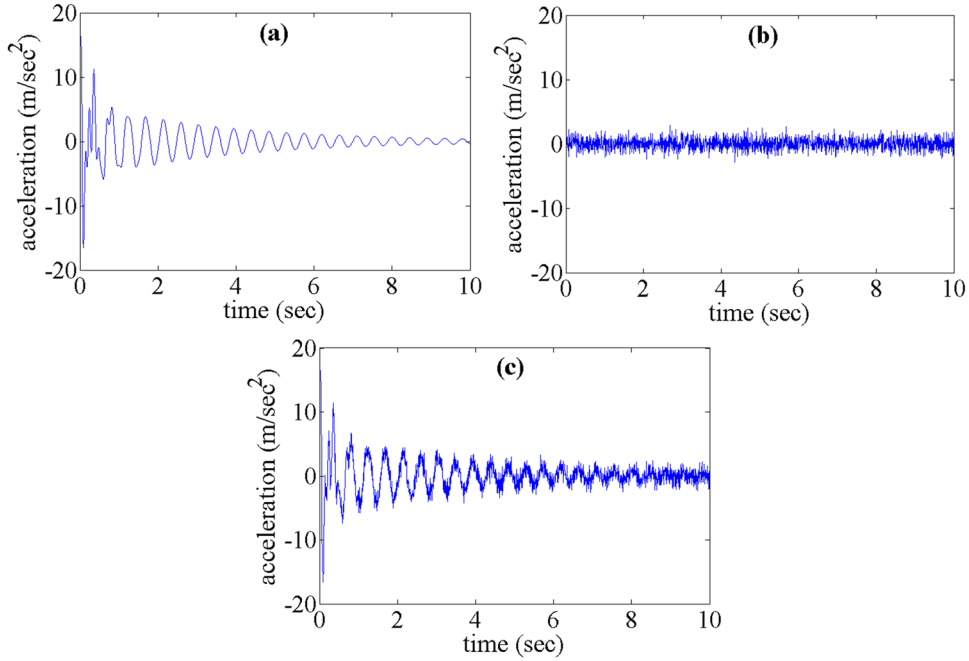

Figure 2. (a) Acceleration response of the third DOF; (b) simulated noise; (c) noisy measurement.

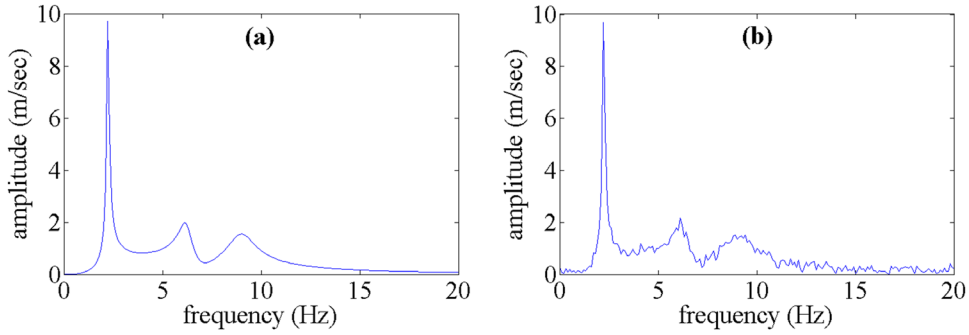

Figure 3. Fourier spectrum of the third DOF measurement: (a) without noise; (b) with noise.

where N_s and $\bar{z}$ are the signal length and the ensemble average of $z(n)$, respectively. If $\mathrm{SD}_{j+1} > \mathrm{SD}_j$ and $\mathrm{SD}_{j+2} > \mathrm{SD}_{j+1}$, then the sifting process stops and the PF is constructed from the results of the $(j-1)$th iteration. Otherwise, the sifting process continues until j reaches its predefined maximum value.

Modal identification using the proposed method

The equation of motion of an n-DOF structure can be written as equation (13):

$$\mathbf{M}\ddot{\mathbf{x}}(t) + \mathbf{C}\dot{\mathbf{x}}(t) + \mathbf{K}\mathbf{x}(t) = \mathbf{F}(t) \tag{13}$$

where $\mathbf{M}$, $\mathbf{C}$, $\mathbf{K}$ are mass, damping, and stiffness matrices, respectively; $\mathbf{x}(t)$ and $\mathbf{F}(t)$ denote the structural displacement vector and external input force vector, respectively. If the normal modes exist, the equation of motion for the jth mode can be expressed as equation (14):

$$\ddot{q}_j(t) + 2\xi_j\omega_j\dot{q}_j(t) + \omega_j^2 q_j(t) = \mathbf{\Phi}_j^T\mathbf{F}(t)/m_j \tag{14}$$

where $q_j(t)$ is the jth modal response; and ξ_j, ω_j, and m_j are the damping ratio, natural frequency, and modal mass of the jth mode, respectively. Also, $\mathbf{\Phi_j}$ stands for the jth mode shape vector and superscript 'T' denotes the transpose operation. Consequently, the acceleration response at the p DOF, $\ddot{x}_p(t)$, is given by equation (15):

$$\ddot{x}_p(t) = \sum_{j=1}^{n} \phi_{pj}\ddot{q}_j(t) \qquad (p = 1, 2, \ldots, n) \tag{15}$$

where ϕ_{pj} is the pth element of the mode shape vector $\mathbf{\Phi_j}$.

In system identification problems, normally the acceleration response at some DOFs, possibly polluted with noise, are available and the goal is to extract the mode shape vectors ($\mathbf{\Phi_j}$), the damping ratios, and the natural frequency of each mode (ξ_j, ω_j).

In the case of free vibration measurements, the proposed method includes the following steps:

i. The measured response is represented in the frequency domain using a Fourier transform, and some lower and upper limits are determined around each dominant frequency.
ii. According to the lower and upper limits, some appropriate band-pass filters are defined and applied to the original measurement (Yang *et al* 2003).

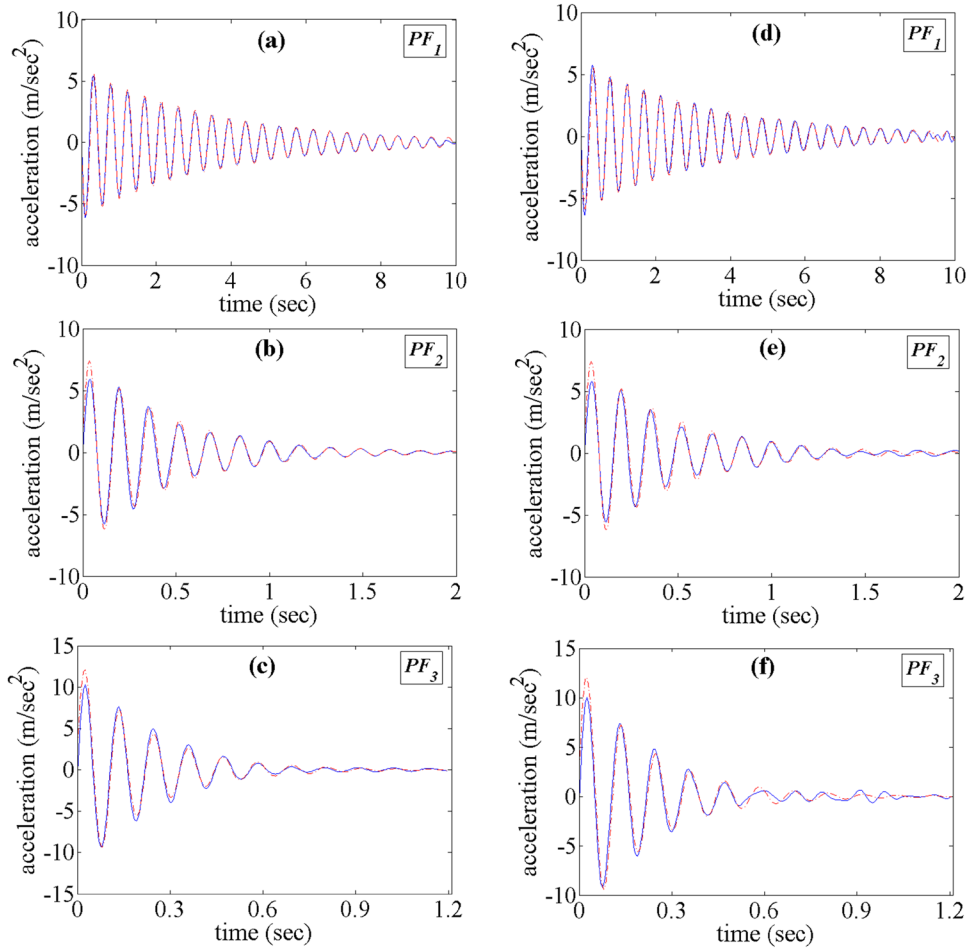

Figure 4. The extracted PFs using the proposed method, along with corresponding exact modal responses; (a)–(c) without noise; (d)–(f) with noise.

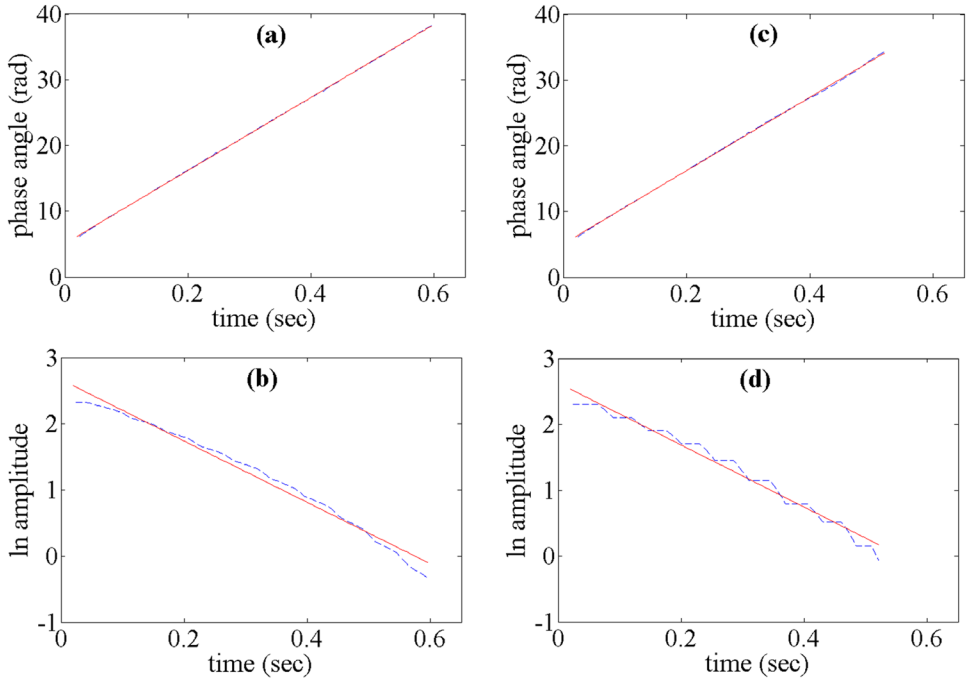

Figure 5. Plots of IP and ln(IA) of the third mode (free vibration test), along with their corresponding fitted lines; (a) and (b) without noise; (c) and (d) with noise.

Table 1. The identification results from the proposed method and the HHT method along with the theoretical values (free vibration test).

Mode number	The proposed method				The HHT method (Yang *et al* 2003)				Theoretical values	
	$R_{nj}=0$		$R_{nj}=5\%$		$R_{nj}=0$		$R_{nj}=5\%$			
	f(Hz)	$\xi(\%)$	f(Hz)	$\xi(\%)$	f(Hz)	$\xi(\%)$	f(Hz)	$\xi(\%)$	f(Hz)	$\xi(\%)$
1	2.22	2.10	2.21	1.98	2.22	2.10	2.21	1.9	2.22	2.00
2	6.21	5.64	6.22	5.47	6.22	5.70	6.19	5.5	6.21	5.60
3	8.88	8.32	8.91	8.43	8.94	7.80	8.94	7.6	8.98	8.10

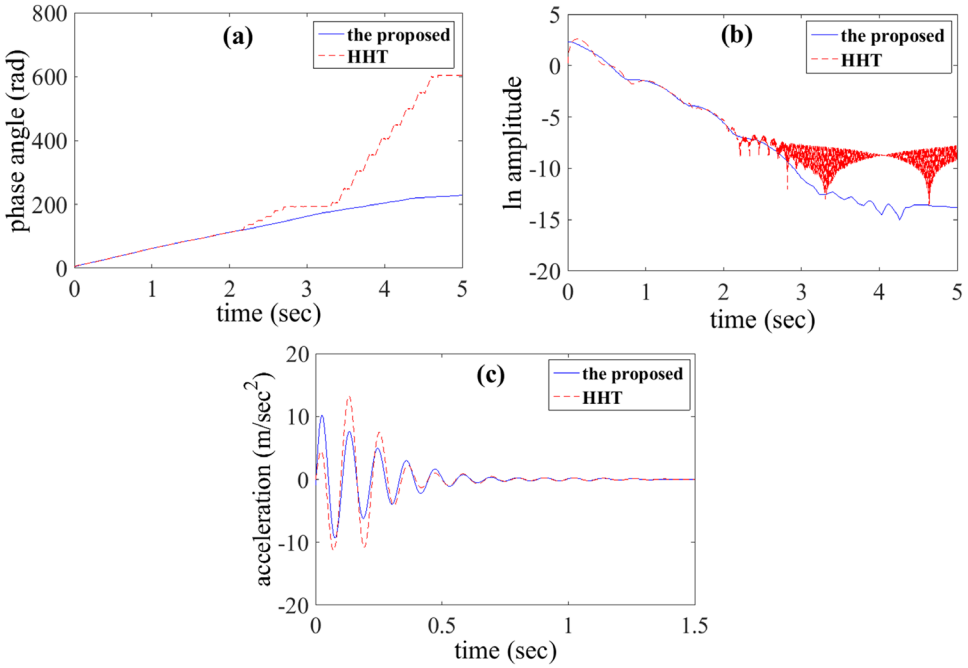

Figure 6. A comparison between plots of: (a) IP, (b) ln(IA), and (c) extracted modal response for the third mode using the proposed method and the HHT method, in a larger time domain.

Table 2. MAC values for identified modes using the proposed method and the HHT method (free vibration test).

Mode	The proposed method		The HHT method	
	$R_{nj}=0$	$R_{nj}=5\%$	$R_{nj}=0$	$R_{nj}=5\%$
1	0.999	0.999	1.00	1.00
2	1.00	1.00	1.00	0.998
3	1.00	0.998	0.999	0.999

iii. The LMD algorithm is applied to the filtered responses to extract corresponding PFs. Also, the instantaneous amplitudes, IAs, and the instantaneous phase angles, IPs, are obtained.

iv. For the jth extracted PF, the slope of the corresponding IP and ln(IA) versus the time plots gives the damped natural frequency, ω_{dj}, and $-\xi_j\omega_j$, respectively. The linear least-squares fitting procedure is used in this step.

v. To identify the mode shape vectors, the measurements in all DOFs are required. If so, the absolute values and the signs of the elements of the jth mode shape vector, relative to an arbitrary element, can be determined by equations (16a) and (16b), respectively (Yang *et al* 2003):

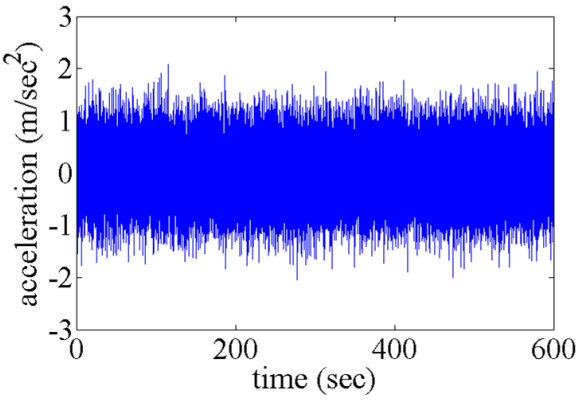

Figure 7. Simulated ambient base excitation for case study (I).

$$|\phi_{pj}| / |\phi_{qj}| = \exp\left[\mathrm{IA}'_{pj}(t_0) - IA'_{qj}(t_0)\right] \tag{16a}$$

$$\varphi_{pj,q} = IP'_{pj}(t_0) - IP'_{qj}(t_0) \tag{16b}$$

where ϕ_{pj}, ϕ_{qj} are the pth and qth elements of the mode shape vector $\mathbf{\Phi_j}$ respectively; $\varphi_{pj,q}$ is the difference between phase angle of the above modal elements; $\mathrm{IA}'_{xy}(t_0)$ and $\mathrm{IP}'_{xy}(t_0)$ are, respectively, the values of the straight lines fitted to ln(IA) and

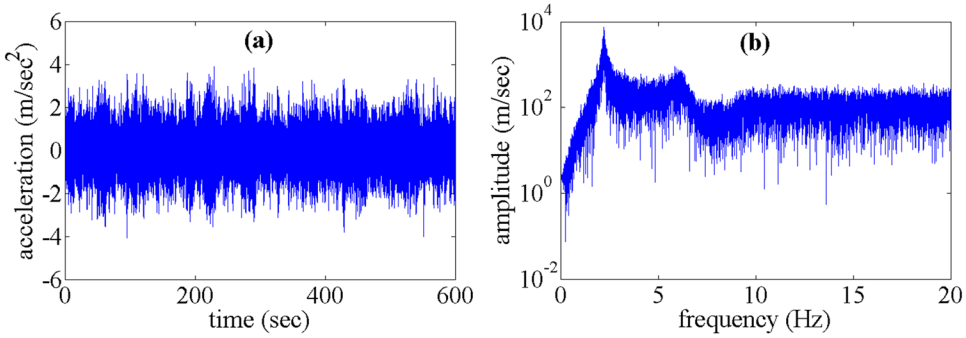

Figure 8. (a) Acceleration response in the third DOF; (b) corresponding Fourier spectrum.

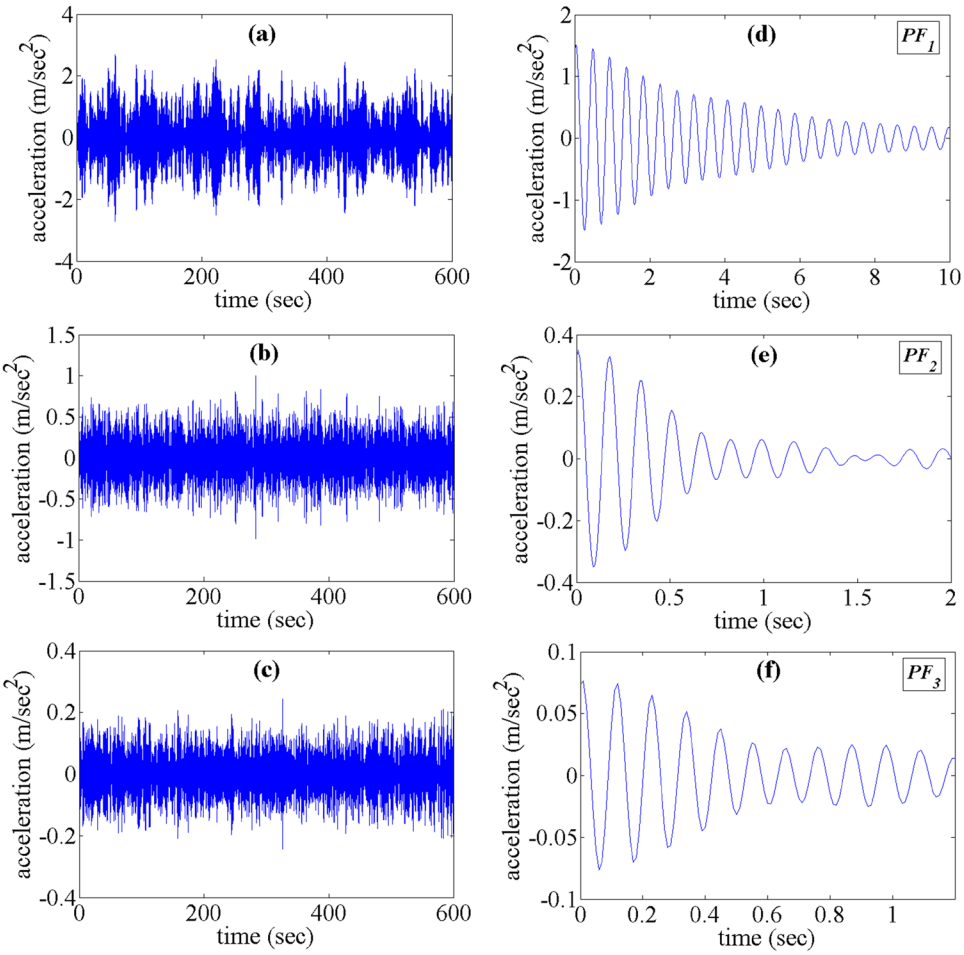

Figure 9. (a)–(c) Filtered responses of third DOF measurement due to ambient base excitation; (d)–(f) the extracted PFs.

IP versus the time plots at time instant t_0; and the subscripts 'pj' and 'qj' indicate that the values are related to the jth mode identified by the measurement at pth and qth DOFs, respectively. It should be remembered that in the case of normal modes, the value of $\varphi_{pj,q}$ is either $\pm 2m\pi$ or $\pm(2m+1)\pi$ (Yang *et al* 2003).

In the case of ambient vibration measurements, the proposed method still works with one modification. In this case, the random decrement technique (RDT) is used to the convert the filtered responses, obtained from step (ii) above, to the corresponding RD signature, which is proportional to the free-decay modal response. The RD signatures are then utilized as inputs for the LMD algorithm in step (iii).

Numerical studies

Case study (I): modal identification of a 3-DOF shear frame

To evaluate the capability of the proposed method in structural identification problems, firstly a 3-DOF shear building structure, as shown in figure 1(a), was considered. The simplified model is illustrated in figure 1(b).

The mass, stiffness and viscous damping of all stories are equal to $m_j = 1000\,\text{kg}$, $k_j = 980\,\text{kN m}^{-1}$, $c_j = 2.814\,\text{kN s m}^{-1}$ $(j = 1, 2, 3)$, respectively (Yang *et al* 2003). According to the recorded responses, the study has been performed in two scenarios: (a) a free vibration test; (b) an ambient vibration

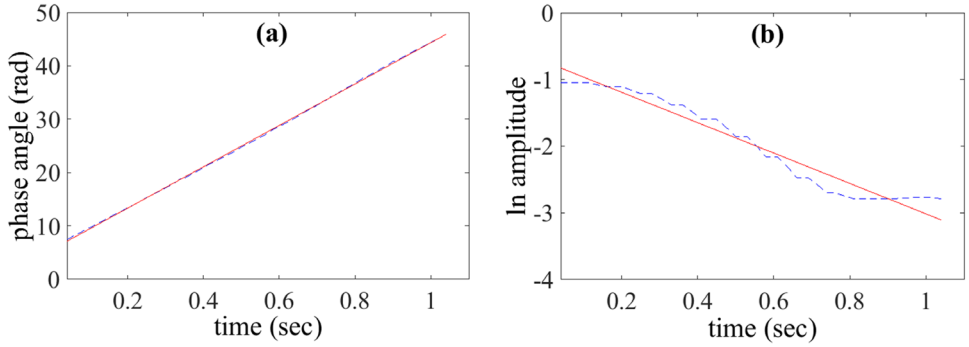

Figure 10. Plots of (a) IP, and (b) ln(IA) for the second mode (ambient vibration test), along with their corresponding fitted lines.

test. In the following, the identification results for each case are considered separately.

Free vibration test. In this phase, an impulse force with a magnitude of 1000 N is applied to the second DOF of the shear frame and the acceleration responses recorded at all DOFs. To examine the noise effect, some white Gaussian noises are simulated and added to each acceleration response. In this study, the noise level is defined as $R_{nj} = \sigma_j / \max|\ddot{x}_j(t)|$ in which σ_j is the root mean square value of the jth simulated noise (we set $R_{nj} = 5\%$ for $j = 1, 2, 3$).

The acceleration response at the third DOF, simulated noise, and corresponding noisy measurement are plotted in figures 2(a)–(c), respectively. Moreover, the Fourier spectra of the measurements in figures 2(a) and (c) are presented in figures 3(a) and (b), respectively.

According to the Fourier spectra in figures 3(a) and (b), there are three dominant frequencies, with the first one around 2 Hz, the second one around 6 Hz, and the third one around 8 Hz. Therefore, the lower and upper limits for the band-pass filtering step, can be determined as follows: $1.8\,\text{Hz} < f_1 = \omega_1/2\pi < 4.3\,\text{Hz}$, $4.3\,\text{Hz} < f_2 = \omega_2/2\pi < 7.7\,\text{Hz}$, $7.7\,\text{Hz} < f_3 = \omega_3/2\pi < 16.7\,\text{Hz}$.

The appropriate band-pass filter is defined for each mode, based on the above limits, and applied to the measurement. Finally, the filtered responses are processed through the LMD algorithm to obtain the corresponding PFs, IPs, and IAs. The extracted PFs from vibration data without and with noise are plotted in figures 4(a)–(f), respectively. In these figures, the red dashed curves show the exact acceleration modal responses. It should be noted that the extracted PF_j corresponds to the modal response, $\ddot{q}_j(t)$.

The plots of IP_3 and $\ln(\text{IA}_3)$ versus the time along with their corresponding fitted lines, without and with noise, are shown in figures 5(a)–(d), respectively.

It should be noted that, as seen in figures 3(a) and (b), participation of the third mode in the measurement is the lowest one. Therefore, the identification results (PF, IP, IA) for this mode have more errors.

The identification results obtained from the proposed method and the HHT method, for the without and with noise cases, along with the theoretical values are illustrated in table 1. As seen, the natural frequencies of all modes have been extracted with high accuracy using both HHT and the proposed methods. However, the accuracy of the estimated damping ratios using both methods decreases for third mode. Also, the additive noise in the measurements has no significant effect on the identification results.

Table 3. The identification results for the three-storey shear frame subjected to ambient base excitation.

	The proposed method		The HHT method		Theoretical values	
Mode	f(Hz)	$\xi(\%)$	f(Hz)	$\xi(\%)$	f(Hz)	$\xi(\%)$
1	2.23	2.02	2.23	2.51	2.22	2.0
2	6.19	5.86	6.21	5.38	6.21	5.6
3	9.14	3.79	9.24	4.61	8.98	8.1

For a more realistic comparison between two methods, the plots of IP, IA, and the extracted modal response are respectively shown in figures 6(a)–(c) in a larger time domain (only the results for third mode are shown here).

As seen in figures 6(a)–(c), the end effect issue is more restricted in the proposed method rather than the HHT one. Also, the proposed method shows fewer deviations from linear form, in both plots of $\text{IP}_3(t)$ and $\ln(\text{IA}_3(t))$, rather than the HHT method. Since the estimated natural frequencies and damping ratios in table 1 were obtained using only small parts of the corresponding curves between two time points, more cautions should be taken for selection of these time points to have reasonable accuracy when using the HHT method.

In addition, the mode shape vectors can be identified by equations (16*a*) and (16*b*). An almost modal assurance criterion (MAC), defined by equation (17), is used to evaluate the accuracy of the identified mode shape vectors:

$$\text{MAC}_i = \frac{\left(\phi_i^T \bar{\phi}_i\right)^2}{\left(\phi_i^T \phi_i\right)\left(\bar{\phi}_i^T \bar{\phi}_i\right)} \tag{17}$$

where ϕ_i and $\bar{\phi}_i$ represent the theoretical and estimated ith mode shape vector, respectively.

The MAC values of the identified mode shape vectors are presented in table 2, for $R_{nj} = 0$ and $R_{nj} = 5\%$. As seen, all of the mode shape vectors were identified exactly using both HHT and the proposed methods. However, the accuracy of the HHT method slightly reduces for higher modes.

Ambient vibration test. In this section, the 3-DOF shear frame is subjected to an ambient base excitation. As shown in figure 7, ambient excitation is simulated as a white noise. The

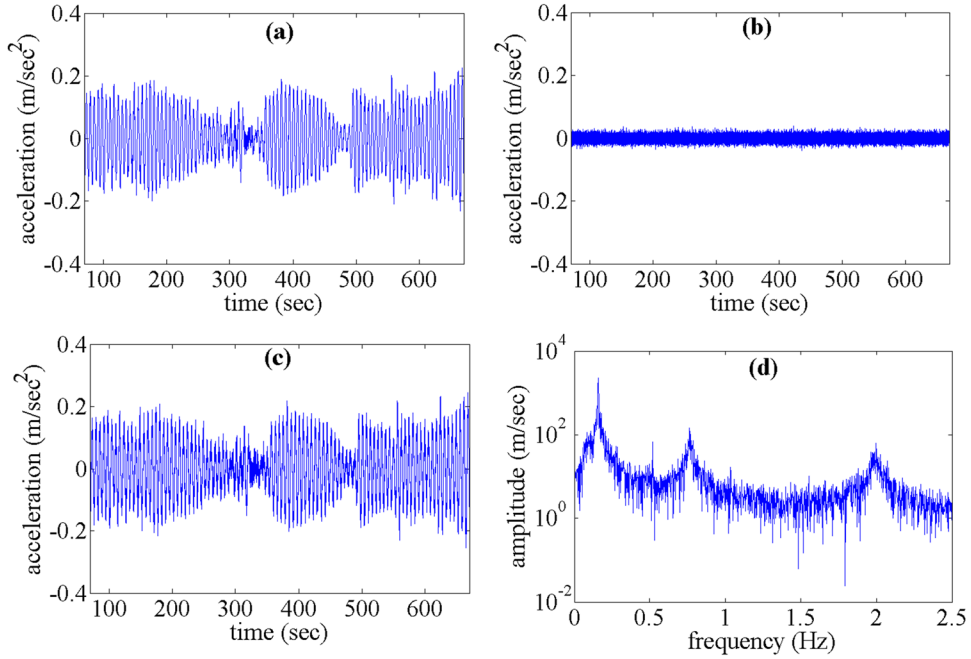

Figure 11. (a) Top floor acceleration response of the benchmark building due to wind excitation; (b) simulated noise; (c) measurement response, $\ddot{z}_{76}$; (d) Fourier spectrum of $\ddot{z}_{76}$.

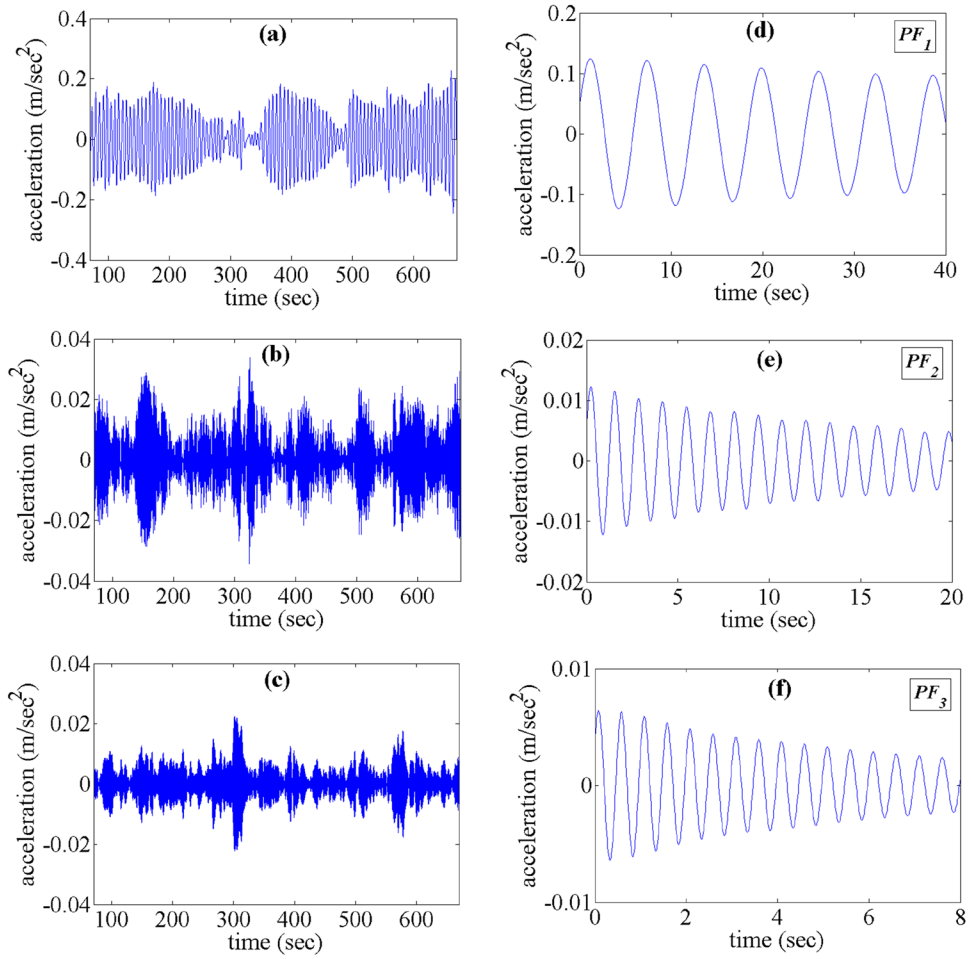

Figure 12. (a)–(c) Plots of filtered responses; (d)–(f) the extracted PFs.

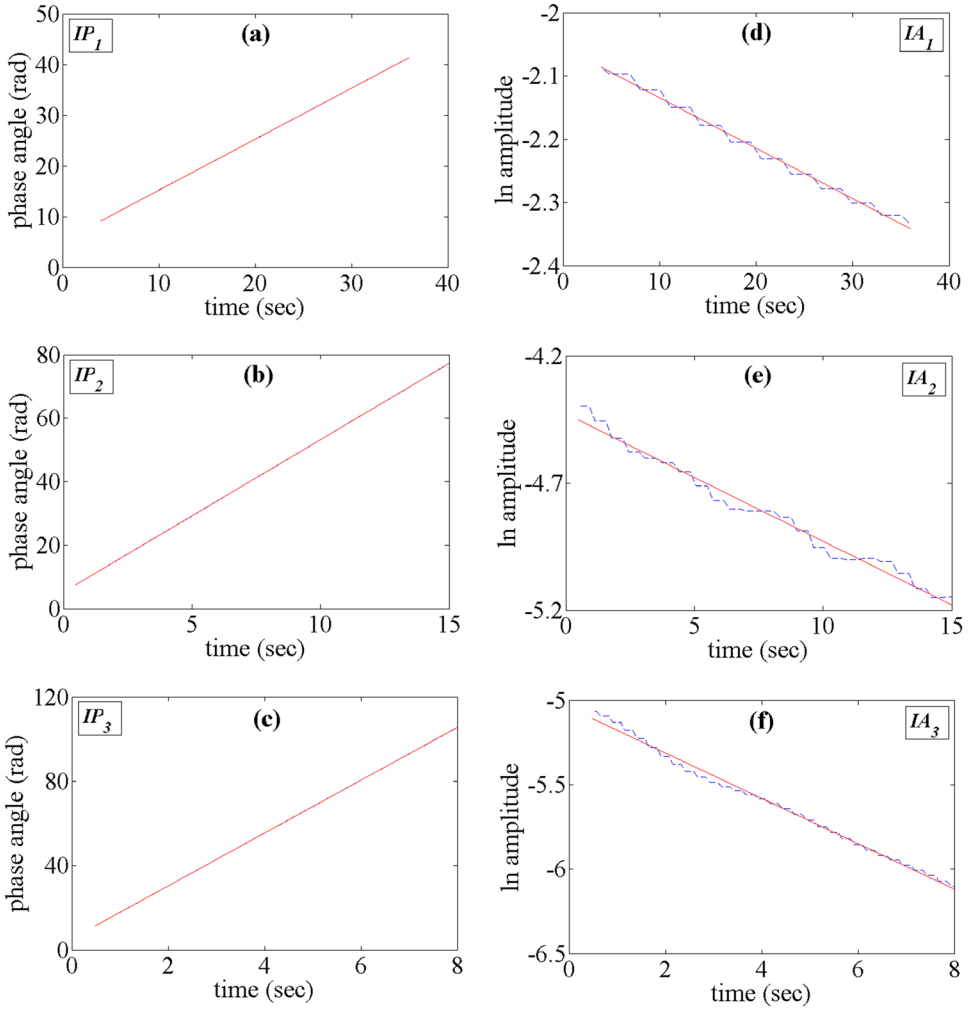

Figure 13. Plots of (a)–(c) IP, and (d)–(f) ln(IA) for three identified modes from noisy measurement, along with their corresponding fitted lines.

third DOF acceleration response and corresponding Fourier spectrum are plotted in figures 8(a) and (b), respectively.

As observed in figure 8(b), the participation of the third mode in the measured response is very low. Therefore, it can be expected that the identification results for the third mode have less accuracy than the first two modes.

However, the band-pass filters defined for the free vibration test are also used in this section. Subsequently, the RDT should be applied on the filtered responses before processing by the LMD algorithm. To this aim, the triggering levels are determined as $[0.5\sigma, +\infty]$, where σ is the standard deviation of each filtered response. The filtered responses and the extracted PFs are shown in figures 9(a)–(f), respectively.

Due to brevity, only plots of IP_2 and $\ln(\mathrm{IA}_2)$ versus the time along with their corresponding fitted lines are shown in figures 10(a) and (b), respectively. Finally, the natural frequencies, damping ratios, for identified modes by both HHT and the proposed method, are summarized in table 3. As presented, the proposed method identifies the natural frequencies accurately, even for the third mode. However, the accuracy of the estimated damping ratio of the third mode is very low, as expected. It should be noted that the traditional RD technique, used in the proposed method, disturbs the mode shape information in the measurements. Therefore, the MAC values in the ambient vibration test are not presented here.

Case study (II): modal identification of an in situ tall building from ambient wind vibrations

Yang *et al* (2004b) conducted a study on the identification of a 76-storey benchmark building using the HHT method. In this section, the proposed identification method is applied to this building response as a validation study. The building considered is a concrete tower with 76 storeys, 306.1 m in height and 42 m in width, proposed for the city of Melbourne, Australia. Due to its slenderness (aspect ratio of 7.3), the building is sensitive to wind excitations (Yang *et al* 2004a). Different control strategies were applied on this benchmark building to reduce the responses due to wind excitation. Wind tunnel tests were conducted for this building and the wind forces and responses in all storeys were measured. More detail of this benchmark problem can be found in Yang *et al* (2004a) and (2004b).

In this case study, the noise level is defined as $R_n = \sigma_v/\sigma_{\ddot{x}}$, where $\sigma_v, \sigma_{\ddot{x}}$ are root-mean squares of noise and acceleration response, respectively. Considering $R_n = 10\%$, a white Gaussian noise, v, is simulated and added to the top

Table 4. The identification results from the proposed method and those from the HHT method, along with the theoretical values for case study (II).

Mode Number	The proposed method				The HHT method (Yang *et al* 2004b)				Theoretical values	
	$R_n = 0$		$R_n = 10\%$		$R_n = 0$		$R_n = 10\%$			
	f(Hz)	$\xi(\%)$	f(Hz)	$\xi(\%)$	f(Hz)	$\xi(\%)$	f(Hz)	$\xi(\%)$	f(Hz)	$\xi(\%)$
1	0.16	0.99	0.16	0.99	0.16	1.03	0.16	0.91	0.16	1.00
2	0.76	1.05	0.76	1.04	0.77	1.06	0.77	1.06	0.76	1.00
3	1.99	1.01	1.99	1.07	1.98	0.95	1.98	1.00	1.99	1.00

floor acceleration response, $\ddot{x}_{76}$, to obtain the noisy measurement, $\ddot{z}_{76} = \ddot{x}_{76} + v$. Plots of $\ddot{x}_{76}$, v and $\ddot{z}_{76}$, are shown in figures 11(a)–(c), respectively. To ensure a steady state response, only the time history response in the range [70 670] seconds is considered for subsequent analyses.

In addition, the Fourier spectra of $\ddot{z}_{76}$, is plotted in figure 11(d). As seen, there are three dominant frequencies around 0.15 Hz, 0.75 Hz, and 2 Hz, respectively. Therefore, the following limits are considered to define band-pass filters for both the without and with noise cases: $0.1\,\text{Hz} < f_1 = \omega_1/2\pi < 0.25\,\text{Hz}$; $0.5\,\text{Hz} < f_2 = \omega_2/2\pi < 1\,\text{Hz}$;$1.7\,\text{Hz} < f_3 = \omega_3/2\pi < 2.3\,\text{Hz}$.

Now the RDT is used to convert each filtered response to the corresponding RD signature, which is proportional to the free-decay modal response. To this aim, the triggering levels are determined as $[0.3\sigma, +\infty]$, where σ is the standard deviation of each filtered response. Then the LMD algorithm is applied to the RD signatures to extract the corresponding natural frequencies and damping ratios. The filtered responses and the corresponding extracted PFs from noisy measurement are shown in figures 12(a)–(f), respectively.

Figures 13(a)–(f) show, respectively, plots of $\text{IP}(t)$ and $\ln(\text{IA}(t))$ for the extracted modes from noisy measurement. Also, the solid red lines in these figures indicate the fitted ones using the linear least squares fitting procedure.

The natural frequencies and damping ratios extracted using the proposed method, the HHT method, and the theoretical values are summarized in table 4.

As presented, the natural frequencies extracted by both of the proposed method and the HHT method are exact, but the accuracy of the identified damping ratios reduces for higher modes. Moreover, the additive noise in the measurements has no significant effect on the identification results.

Conclusion

In this paper, the LMD algorithm was investigated as a possible candidate for modal identification of civil structures. In this way, a new method, based on the LMD algorithm, was proposed and its ability examined by some numerical studies. For better insight, the identification results from the proposed method were compared with those from the HHT method. The following conclusions can be highlighted from this study:

- Only one measurement is required for identification of natural frequencies and damping ratios of all active modes by the proposed method. However, for extracting the mode shape vectors, the measurements of all DOFs are required.
- In both cases of free vibration and ambient vibration, the natural frequencies extracted by the proposed method, in both without and with noise cases, have reasonable accuracy. However, the accuracy of the identified damping ratios reduces for higher modes.
- While an additional Hilbert transform is required to obtain the IA and the IP in the EMD algorithm, these functions are directly obtained during the sifting process of the proposed method.
- The IP and natural logarithm of the IA curves obtained by the proposed method show more linearity for a larger time domain in comparison with those obtained by the HHT method.
- The end effect issue is more restricted for the proposed method in comparison with the HHT method.
- The additive noise in the measurements has no significant effect on the identification results of the proposed method.

Acknowledgments

This research received no specific grant from any funding agency in the public, commercial, or not-for-profit sectors. The authors would like to appreciate the general support of Shahrood University of Technology and to thank the anonymous reviewers for their constructive comments, which helped improve the article. Finally, the authors declare no conflict of interest in preparing this article.

ORCID iDs

Saeed Mohammadi https://orcid.org/0000-0002-7611-8596

References

Abdelghani M, Verhaegen M, Van Overschee P and De Moor B 1998 Comparison study of subspace identification methods applied to flexible structures *Mech. Syst. Signal Process.* **12** 679–92

Cheng J, Yang Y and Yang Y 2012 A rotating machinery fault diagnosis method based on local mean decomposition *Digit. Signal Process.* **22** 356–66

Hazra B, Sadhu A, Roffel A J, Paquet P E and Narasimhan S 2012 Under-determined blind identification of structures by

using the modified cross-correlation method *J. Eng. Mech.* **138** 327–37
Huang N E, Shen Z, Long S R, Wu M C, Shih H H, Zheng Q, Yen N, Tung C C and Liu H H 1998 The empirical mode decomposition and the Hilbert spectrum for nonlinear and non-stationary time series analysis *Proc. R. Soc.* A **454** 903–95
Ibrahim S R and Mikulcik E C 1973 A time domain modal vibration test technique *Shock Vib. Bull.* **43** 21–37
James G H, Carne T G and Lauffer J P 1995 The natural excitation technique (NExT) for modal parameter extraction from operating structures *Modal Anal.* **10** 260–77
Juang J N and Pappa R S 1985 An eigen system realization algorithm for modal parameter identification and model reduction *J. Guid. Control Dyn.* **8** 620–7
Kerschen G, Poncelet F and Golinval J C 2007 Physical interpretation of independent component analysis in structural dynamics *Mech. Syst. Signal Process.* **21** 1561–75
Li Z, Park H S and Adeli H 2017 New method for modal identification of super high-rise building structures using discretized synchrosqueezed wavelet and Hilbert transforms *Struct. Design Tall Spec. Build.* **26** e1312
Liu H and Han M 2014 A fault diagnosis method based on local mean decomposition and multi-scale entropy for roller bearings *Mech. Mach. Theory* **75** 67–78
Liu Z, Jin Y, Zuo M J and Feng Z 2017 Time-frequency representation based on robust local mean decomposition for multicomponent AM–FM signal analysis *Mech. Syst. Signal Proces.* **95** 468–87
Perez-Ramirez C A *et al* 2016 New methodology for modal parameters identification of smart civil structures using ambient vibrations and synchrosqueezed wavelet transform *Eng. Appl. Artif. Intell.* **48** 1–12
Quek S T, Tua P S and Wang Q 2003 Detecting anomalies in beams and plate based on the Hilbert–Huang transform of real signals *Smart Mater. Struct.* **12** 447–60
Sadhu A 2017 An integrated multivariate empirical mode decomposition method towards modal identification of structures *J. Vib. Control* **23** 2727–41
Sadhu A, Narasimhan S and Antoni J 2017 A review of output-only structural mode identification literature employing blind source separation methods *Mech. Syst. Signal Process.* **94** 415–31
Smith S 2005 The local mean decomposition and its application to EEG perception data *J. R. Soc. Interface* **2** 443–54
Wang Y, He Z and Zi Y 2009 A demodulation method based on improved local mean decomposition and its application in rub-impact fault diagnosis *Meas. Sci. Technol.* **20** 025704
Wu Z and Huang N E 2009 Ensemble empirical mode decomposition: a noise-assisted data analysis method *Adv. Adapt. Data Anal.* **01** 1–41
Xiang L and Yan X 2014 A self-adaptive time-frequency analysis method based on local mean decomposition and its application in defect diagnosis *J. Vib. Control* **22** 1049–61
Yang J N, Agrawal A K, Samali B and Wu J C 2004a Benchmark problem for response control of wind-excited tall buildings *J. Eng. Mech.* **130** 437–46
Yang J N, Lei Y, Lin S and Huang N 2004b Identification of natural frequencies and dampings of *in situ* tall buildings using ambient wind vibration data *J. Eng. Mech.* **130** 570–7
Yang J N, Lei Y, Pan S and Huang N 2003 System identification of linear structures based on Hilbert–Huang spectral analysis. Part 1: normal modes *Earthq. Eng. Struct. Dyn.* **32** 1443–67